ARMY RESEARCH LABORATORY

The Design of Accurate Micro-compression Experiments

by Haitao Zhang, Brian E. Schuster, Qiuming Wei, and Kaliat T. Ramesh

NOTICES

Disclaimers

The findings in this report are not to be construed as an official Department of the Army position unless so designated by other authorized documents.

Citation of manufacturer's or trade names does not constitute an official endorsement or approval of the use thereof.

Destroy this report when it is no longer needed. Do not return it to the originator.

Army Research Laboratory

Aberdeen Proving Ground, MD 21005-5066

The Design of Accurate Micro-compression Experiments

Brian E. Schuster
Weapons and Materials Research Directorate, ARL

Haitao Zhang, Qiuming Wei, and Kaliat T. Ramesh
The Johns Hopkins University

REPORT DOCUMENTATION PAGE

Form Approved
OMB No. 0704-0188

1. REPORT DATE (DD-MM-YYYY)	2. REPORT TYPE	3. DATES COVERED (From - To)
January 2006	Reprint	January–June 2005

4. TITLE AND SUBTITLE	5a. CONTRACT NUMBER
The Design of Accurate Micro-compression Experiments	
	5b. GRANT NUMBER
	5c. PROGRAM ELEMENT NUMBER

6. AUTHOR(S)	5d. PROJECT NUMBER
Haitao Zhang,[*] Brian E. Schuster, Qiuming Wei,[*] and Kaliat T. Ramesh[*]	58T8G7
	5e. TASK NUMBER
	5f. WORK UNIT NUMBER

7. PERFORMING ORGANIZATION NAME(S) AND ADDRESS(ES)	8. PERFORMING ORGANIZATION REPORT NUMBER
U.S. Army Research Laboratory ATTN: AMSRD-ARL-WM-TC Aberdeen Proving Ground, MD 21005-5066	ARL-RP-114

9. SPONSORING/MONITORING AGENCY NAME(S) AND ADDRESS(ES)	10. SPONSOR/MONITOR'S ACRONYM(S)
	11. SPONSOR/MONITOR'S REPORT NUMBER(S)

12. DISTRIBUTION/AVAILABILITY STATEMENT

Approved for public release; distribution is unlimited.

13. SUPPLEMENTARY NOTES

14. ABSTRACT

We investigate (via finite-element analyses) the factors that may affect the accuracy of micro-compression measurements. Based on these simulations, we suggest guidelines for the development of accurate micro-compression experiments in terms of fillet to post radius ratio, post aspect ratio, post taper, and system alignment.

15. SUBJECT TERMS

micro-mechanics, constitutive behavior, finite element modeling, buckling, specimen geometry, micro-compression

16. SECURITY CLASSIFICATION OF:			17. LIMITATION OF ABSTRACT	18. NUMBER OF PAGES	19a. NAME OF RESPONSIBLE PERSON Brian Schuster
a. REPORT UNCLASSIFIED	b. ABSTRACT UNCLASSIFIED	c. THIS PAGE UNCLASSIFIED	UL	12	19b. TELEPHONE NUMBER (Include area code) 410-278-6733

Standard Form 298 (Rev. 8/98)
Prescribed by ANSI Std. Z39.18

ELSEVIER

Scripta MATERIALIA

The design of accurate micro-compression experiments

H. Zhang [a], B.E. Schuster [a,b], Q. Wei [a], K.T. Ramesh [a,*]

[a] *Department of Mechanical Engineering, The Johns Hopkins University, Baltimore, MD 21218, USA*
[b] *Army Research Laboratory, Weapons and Materials Research Directorate, Aberdeen Proving Ground, MD 21005, USA*

Abstract

We investigate (via finite-element analyses) the factors that may affect the accuracy of micro-compression measurements (see, e.g., Uchic et al. [Uchic MD, Dimiduk DM, Florando JN, Nix WD. Science 2004;305:986]). Based on these simulations, we suggest guidelines for the development of accurate micro-compression experiments in terms of fillet to post radius ratio, post aspect ratio, post taper, and system alignment.

1. Introduction

Current commercial nano-indenters have sub-nanometer displacement resolution under ideal conditions (perhaps reduced to ∼0.1 nm due to thermal drift and noise), and a load resolution better than 1 nano-newton. This high precision makes the technique popular in many applications such as the measurement of mechanical properties of very thin films and tribological measurements of coatings. In a conventional nano-indentation experiment, a Berkovich tip is used to probe the nano-scale mechanical behavior (such as hardness and elastic modulus) as a function of indentation depth. For example, it was found that the indentation size has a strong effect on the hardness of single crystal silver [2]. Recently, a modified tip geometry has been utilized to probe the nano-scale mechanical behavior of micro-scale or even sub-micro pillars [1,3,4]. In this modification, the sharp Berkovich tip is truncated, resulting in a flat ended tip and converting the indentation system into a compression system. This technique is commonly called "micro-compression" or μ-compression, and has been used for the investigation of specimen size

effects on the mechanical properties of single crystals of metals and alloys [1,3,4]. Although these previous works are for single crystals or large crystals where crystal anisotropy is significant, we are interested also in the application of this technique to isotropic materials, e.g., nano-structured materials and metallic glasses. This approach may be effective for many advanced materials which are difficult to obtain in bulk form, and whose tensile ductility is limited (so that micro-tension tests are difficult). For example, it is currently extremely difficult to produce bulk forms of many metals and ceramics with nano-crystalline micro-structure [5,6]. Nevertheless, they can be readily produced in thin foils and small cubes or cylinders with dimensions less than 1 mm [7]. Further, advanced technologies such as micro-electromechanical and/or nano-electromechanical systems (MEMS, NEMS) require knowledge of the mechanical properties of the materials used to fabricate such systems [8]. Conventional mechanical testing techniques are not useful due to the small size of specimens.

Micro-compression makes use of a conventional nano-indenter and a flat-end tip, to measure the stress–strain curves of materials using posts as small as 200–300 nm in diameter [4]). Technologies such as focused ion beams (FIB) enable researchers to fabricate such posts with ease. However, these posts usually have one end (the bottom)

---

* Corresponding author. Tel.: +1 410 516 7735; fax: +1 410 516 7254.
E-mail address: ramesh@jhu.edu (K.T. Ramesh).

fixed on the matrix (or the base material), while the top end is pressed by the flat-end tip during a μ-compression experiment. To what extent can the data from such micro-scale measurements be used to represent the macro-scale materials behavior? In this work, we present a parametric study of the design of accurate μ-compression experiments using two-dimensional (2D) and three-dimensional (3D) finite element modeling. We consider geometric factors such as the fillet radius (or the curvature at the bottom of the post connecting to the base), and the aspect ratio of the post (defined as the height/diameter ratio), as well as materials properties such as strain hardening and strain rate sensitivity. The 3D model is used to examine plastic buckling phenomena, and the effect of post taper and misalignment of the system on the accuracy of measurement. The numerical results presented here can serve as guidelines for the implementation of μ-compression experiments on various materials. We find that μ-compression can be used to measure the mechanical properties of mechanically isotropic materials (such as nano-structured materials and metallic glasses) to very good accuracy, as well as to explore size effects in such materials.

2. Modeling and results

In this section, we first use axisymmetric 2D simulations to study the effects of specimen geometry on the output. Next, we examine the effects of friction, post taper, and system misalignment on the buckling of the post using 3D simulations.

2.1. Axisymmetric 2D simulations

Here we consider a post with cylindrical geometry sitting on a base of the same material as shown in Fig. 1(a). In this simplified model we only consider the revolution section (Fig. 1(b)) to simulate the response of the post under compressive loading. A velocity boundary condition corresponding to the imposed strain rate is applied to the post top, and a fixed boundary to the bottom of the base in x_2-direction. The true stress–strain behavior of the post can be obtained from the reaction force **T** generated on the post top and the displacement of the post top, **u**, using the following equations:

$$\bar{\sigma}_2 = \frac{1}{\pi r^2} \int_0^r (T_2)_{x_2=h} \mathrm{d}x_1,$$
$$\bar{\varepsilon}_2 = \ln\left(1 + \frac{u_2}{h}\right), \tag{1}$$

where the subscripts 2 indicate the x_2 components of the corresponding vector. These equations are essentially those used in reducing experimental data.

Simulations are performed using the commercial finite element program ABAQUS (Standard Version 6.4, HKS, Inc., Pawtucket, RI). Eight-node bi-quadratic axisymmetric continuum elements (CAX8R) are used for discretization. A typical finite element mesh that leads to converged results is shown in Fig. 1(b).
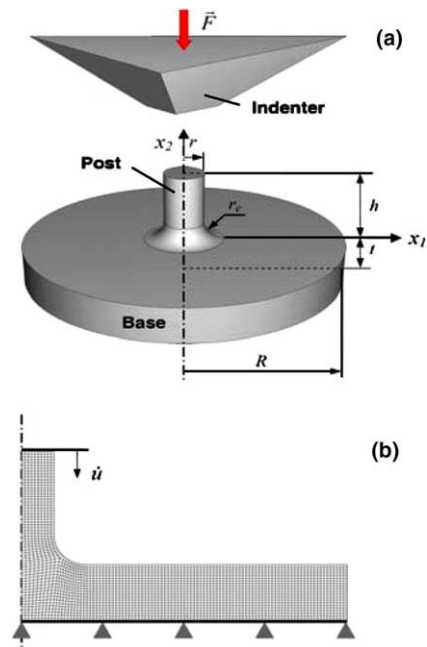

Fig. 1. (a) Schematic of a cylindrical post and its base (made of the same material). In (b), an axisymmetric post model is displayed with the typical finite element discretization used in the 2D simulations.

For simplicity, the input material property of the post is described by the Ramberg–Osgood equation [9]

$$\varepsilon = \frac{\sigma}{E} + \beta\frac{\sigma_0}{E}\left(\frac{\sigma}{\sigma_0}\right)^N, \tag{2}$$

where E is the Young's modulus, N the inverse of the traditional strain hardening exponent, β a material constant and σ_0 a reference stress. We begin with the following parameter set, corresponding to an aluminum (Al) alloy: $E = 70$ GPa, Poisson's ratio $v = 0.33$, $\sigma_0 = 65$ MPa, $\beta = 2.69$, and $N = 4.18$.

The effect of the fillet radius r_c and the post aspect ratio ($\alpha = h/2r$) on the output stress–strain curves are investigated first. We begin by fixing $\alpha = 2$ and varying r_c (expressed in terms of the post radius r). Fig. 2(a) displays the input stress–strain curve from Eq. (2), along with the output stress–strain curves from the simulations with different fillet radii ($r_c = 0.1r$, $0.2r$, $0.5r$ and r). For clarity, a portion of the curves has been enlarged in the inset of Fig. 2(a). Due to the fixed end effect, all the simulated output curves are above the input curve, indicating an overestimate of the flow stress of the material in the plastic range, and the strength of this effect depends on the fillet radius/post radius ratio. The larger the fillet size (with respect to the post radius), the greater the error. When the fillet radius ratio is less than 0.5, the output curves are very close (within 3%) to the input data. This suggests that if the fillet size is well controlled the fixed-end compression measurements can still be used to represent the bulk materials behavior in terms of flow stress. For the aspect ratio $\alpha = 2$, even with the largest fillet radius/post radius ratio, i.e., $r_c/r = 1$, the error in flow stress from the μ-compression test is less than 6%.
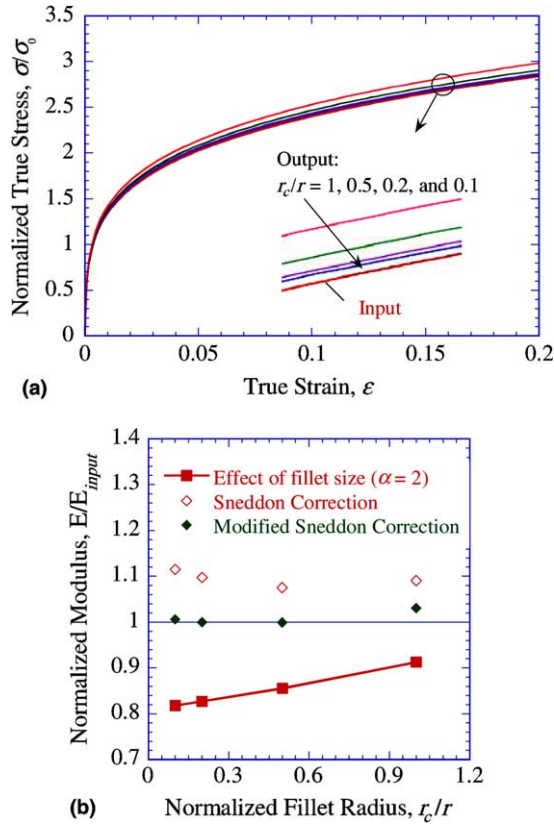
Fig. 2. (a) Effect of specimen geometry (fillet size) on numerical simulation output. The input stress–strain curve is calculated using Eq. (2), and the output stress–strain curves from finite element analysis. The inset shows an enlargement of the circled region to facilitate comparison. The different output curves correspond to different fillet radius/post radius ratios (values are given in the inset). (b) Effects of fillet size on the accuracy of elastic modulus measurements. In (b), we also include the data from the Sneddon and modified Sneddon corrections (see text for details).

The distribution of the von Mises stresses in the post and the base (not shown here) for various fillet radius/post radius ratios shows that with increased fillet size, the stress concentration at the fillet is alleviated. For $r_c/r \geqslant 0.5$, there is no significant stress concentration at the fillet, the maximum von Mises stress being along the post axis. Excessive stress concentrations may result in localized specimen failure prior to general yielding. Thus, the choice of fillet radius for an experiment represents a compromise between the need to accurately recover material behavior in the plastic range (requiring small r_c/r) and the desire to avoid localized failure at the post root (which requires large r_c/r). Our simulations suggest that a choice of r_c/r in the range of 0.2–0.5 represents a good compromise. In practice, the fillet size can be controlled by the FIB or micro-machining parameters. Therefore, we believe it is realistic to use μ-compression to probe the mechanical properties of materials whose constitutive response is described by the generic constitutive equation of Eq. (2).

The second important geometric factor that may affect the accuracy of the measurement is the aspect ratio of the post. In the 2D simulations, the aspect ratio of the posts has a relatively small effect on the output flow stress curves

if the aspect ratio is larger than 2. Aspect ratios of less than 2 are not appropriate, since the output strain hardening of the post material then deviates from the input value due to the constraints from the post base. Buckling and the effect of friction are considered in the later section on 3D simulations.

In a standardized mechanical experiment the machine compliance is eliminated by using extensometers or strain gages and the elastic modulus of the specimen material can then be calculated. But for micro-compression, this type of compliance correction is not possible. Therefore, it is important to examine the factors that will affect the accuracy of elastic modulus measurement. [The work of Chau [10] shows that for aspect ratios $h/2r \geqslant 2$ (desirable for micro-compression experiments), the effect of end friction on the modulus measurement is small (<0.5%)]. We focus, therefore, on geometric effects. Fig. 2(b) displays the error of elastic modulus measurements as a function of the fillet size (the elastic modulus is normalized by the known input modulus). The post aspect ratio is fixed at 2. It is apparent that increased fillet size improves the accuracy with which the elastic modulus is measured, but still underestimates the modulus. The reason is that the base will always deform along with the post, and this deformation contributes to the system compliance, which is not accounted for when collecting the displacement data. However, this error may be alleviated by accounting for the base compliance using a result from Sneddon [11]. Sneddon computed the depth of penetration D of an elastic half-space by a flat-ended rigid cylinder of radius a under a load P as

$$D = \frac{P(1-v)}{4Ga}, \qquad (3)$$

where G and v are, respectively, the shear modulus and Poisson's ratio of the half-space. We then obtain the base compliance [4] as

$$C_b = \frac{1-v}{4Ga} = \frac{1-v^2}{2Ea_c}, \qquad (4)$$

where we have set $a = a_c$, and a_c is the effective contact radius ($a_c = \eta(r + r_c)$, with η a constant chosen to account for the more complex geometry of the post-base connection). By subtracting this base compliance from the total compliance, a corrected post stiffness (and hence modulus) is obtained. If $\eta = 1$ (the Sneddon correction), the modulus is overestimated. We find that setting $\eta = 1.42$ provides a significantly improved correction (we call this the modified Sneddon correction). In Fig. 2(b), we also include both the Sneddon and modified Sneddon corrections. The choice of a in Eq. (4) is difficult because of the geometry of the post-base connection. Setting $a = r$ [4] will result in an even higher modulus. Similar results on the error in the modulus measurement have been found with other aspect ratios.

The accuracy of micro-compression measurements may be affected by the properties of the post material: we consider the effects of the strain-hardening exponent and the strain rate sensitivity. Fig. 3(a) shows the input stress–
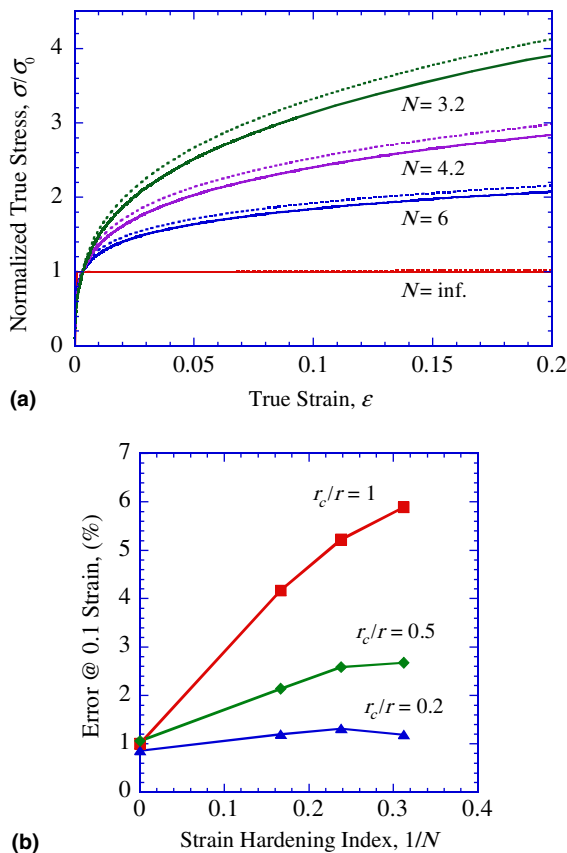
(a)

(b)

Fig. 3. (a) Effect of strain hardening exponent on the error of μ-compression measurement of the stress–strain curve (aspect ratio $\alpha = 2$, and fillet size $r_c = r$). The solid curves are the inputs and the dashed curves are the outputs. (b) The error in flow stress measurement at a fixed strain of 0.1 is plotted against the inverse of N for various fillet sizes (aspect ratio $\alpha = 2$).

strain rate sensitivity of the material [12]. There are various ways to define the strain rate sensitivity. An engineering definition assumes a power-law strain rate hardening such that the strain rate sensitivity is written as $m = \partial \ln \sigma / \partial \ln \dot{\varepsilon}$, where $\dot{\varepsilon}$ is the imposed strain rate. Due to space limitations we do not present the figures in this paper, but our simulations assuming different values of m do indicate that μ-compression can faithfully capture the strain rate sensitivity of the material. Note that the practically useful strain rate achievable for μ-compression with a nano-indenter is probably below $1\ \mathrm{s}^{-1}$, i.e., in the quasistatic regime.

2.2. 3D analyses: buckling, friction, and misalignment

Buckling, either elastic or plastic, is a common concern for a compression test. It is even more of a concern for the μ-compression experiments described in this paper due to the fixed end effect. Therefore, detailed knowledge of the buckling of the sample and the various factors that can contribute to or alleviate such buckling is crucial. Elastic Euler buckling is a trivial calculation, and will not occur even with soft Al posts ($E = 70$ GPa, $\sigma_0 = 65$ MPa) as long as the aspect ratio is below 25. We therefore focus on the plastic buckling problem using 3D finite element analysis. Effects of friction between the indenter (usually made of diamond) and the post top are considered. We also study the effect of "taper" of the post and the system misalignment on the simulation output. The smallest fillet radius ratio used is $r_c/r = 0.1$ for $\alpha = 2$ cylindrical post in the 3D analyses.

Cylindrical and cuboidal posts are used for the numerical 3D simulations. The compression is exerted by a rigid surface representing the flat-end nano-indenter tip. Misalignment of the experimental setup is considered by tilting the rigid surface (perpendicular to the axis of the post for perfect alignment), which can be quantified by the angle θ between the post axis and the rigid surface normal. Like experimental implementations, the displacement of the rigid surface and the force transferred to the post are used to calculate the strain and stress histories of the post. Four-node linear tetrahedron elements (C3D4) are used for discretization. A meshing density that results in numerical convergence is selected.

Simulations are first conducted without considering friction. Fig. 4(a) shows a numerical image of a circular cylindrical Al post with an aspect ratio of 5 at a nominal strain of 0.1. Severe buckling is observed, which affects the experimental stress–strain curve of the post. Fig. 4(c) displays the input and the various outputs assuming different post aspect ratios. This shows that for an aspect ratio of 2 with no friction ($\alpha = 2$, NF), the stress–strain curve does not exhibit leveling off or stress drop due to plastic buckling. However, when the aspect ratio is 5 with no friction ($\alpha = 5$, NF), plastic buckling sets in when the strain is less than 0.02, and the stress starts to level off and gradually decrease.

Friction at the interface of the indenter and the post top is now considered. Micro-compression experiments are usually performed without applying lubrication to the

strain curves calculated using Eq. (2) for different values of the inverse hardening exponent N, and the output stress–strain curves from FE modeling (all curves are normalized by σ_0). In this case, the fillet size is fixed at $r_c = r$ (the worst case) and the posts have an aspect ratio of 2. The input curves are the solid lines, while the output curves are the dashed lines. Fig. 3(a) shows that the error in flow stress from such μ-compression experiments is dependent on the strain hardening behavior of the material. This dependency is better shown by Fig. 3(b) which displays the flow stress error as a function of $1/N$ for a fixed strain of 0.1. Data for smaller fillet sizes, ($r_c = 0.2r$ and $0.5r$) are also shown. The effect of strain hardening on the outputs is reduced when smaller fillet size is used, consistent with our recommended values of r_c/r (0.2–0.5). Fig. 3(b) indicates that the μ-compression technique is most accurate for materials that exhibit low strain hardening. Such materials include nano-structured metals, metals and alloys with ultrafine micro-structure, metallic glasses, and ceramics.

Strain rate effects are also important in many applications, especially when plastic instability is of serious concern. This is because the susceptibility to plastic instability of metals and alloys is strongly dependent on the
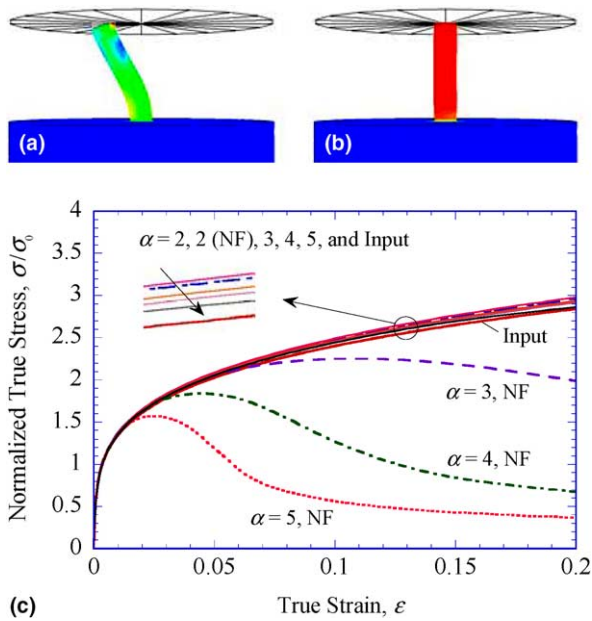
Fig. 4. (a) Deformed configuration of a circular cylindrical post with aspect ratio $\alpha = 5$ at a strain of 0.1, without considering friction. Buckling is severe. (b) Deformed configuration of the post at the same strain of 0.1, now considering friction. No buckling is observed. (c) Input and output stress–strain curves for post aspect ratios $\alpha = 2$–5, both with friction and without friction (NF). Friction effectively suppresses buckling, even for the largest aspect ratio considered ($\alpha = 5$), but further increases the measured flow stress. The arrow in the inset of (c) indicates increasing aspect ratio.

tip-post interface. Our interest is in the effects of friction on buckling and on the fidelity of the technique. A Coulomb friction coefficient μ is used to determine the critical shear stress τ_{crit} from the surface contact pressure p according to $\tau_{crit} = \mu p$. Slipping will occur when τ_{crit} is reached. A range of values for μ exist in the open literature for a number of diamond–metal surface pairs [13]. Typically the static coefficients of friction are in the range of 0.1–0.15, and the kinetic values are 0.03–0.06. A constant $\mu = 0.03$ is selected which is the minimum likely value of the friction coefficient between the diamond indenter tip-post surfaces. Fig. 4(b) shows an image of the same post as shown in Fig. 4(a) at the identical nominal strain of 0.1, but now with friction included in the simulation. No buckling is apparent, and the corresponding stress–strain curve does not exhibit a reduction in stress (indeed, the flow stress is higher than the input). Therefore, friction between the indenter tip and the post top effectively suppresses the plastic buckling of these cylindrical posts, even for the largest aspect ratio considered ($\alpha = 5$). The friction does increase the estimated flow stress. Note that the presence of at least a small amount of friction is intrinsic to these experiments as currently performed. In all of the following results, a friction coefficient of $\mu = 0.03$ is therefore considered, which should be applicable to most experimental conditions.

Another important geometric factor that may have a significant effect on the accuracy of μ-compression experiments is the "taper" of the post (the amount of taper is defined by the tangent of the post wall with respect to the post axis, and

often the top of the post is smaller than the bottom of the post). Taper is typically a result of fabrication inaccuracies. For example, if the beam direction during FIB fabrication is not carefully controlled, one can develop a tapered post. In the following, the effects of taper on the output will be presented. A friction coefficient of 0.03 is used in all of the simulations with taper. The input material behavior is similar to that of a nano-crystalline nickel [14] with an average grain size of ∼20 nm. The material parameters are: $E = 200$ GPa, $v = 0.3$, and a tangent modulus, $E_t = G/200$ is used to represent the plastic response (G is the shear modulus). The results of simulations correspond to prismatic posts with square cross sections, a geometry that we are currently using in micro-compression experiments.

Fig. 5(a) displays the input and the outputs for four conditions: aspect ratio $\alpha = 2$ with and without taper; aspect ratio $\alpha = 5$ with and without taper. The results suggest that when $\alpha = 2$ without taper, the agreement between the output and input is very good (see Fig. 5(a)). However, when the post is tapered with a value of 20:1 (i.e., the angle between the post wall and the post axis is ∼2.86°), first we see that the measured elastic modulus is apparently larger than the input, and then we see a gradual increase of the flow stress after the yielding point (so that the taper of the post produces an artificial strain hardening). This
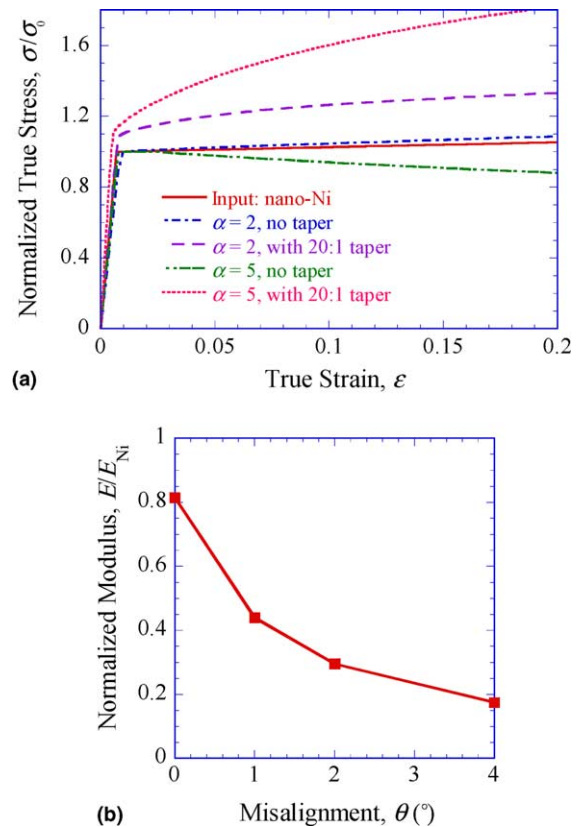

Fig. 5. (a) Effect of post taper and system misalignment on numerical simulation outputs. The amount of taper is defined by the tangent of the post wall to the post axis. (b) The effect of system misalignment on the error in elastic modulus. The zero misalignment condition coincides with the 2D results given in Fig. 2(b).

taper-induced spurious hardening is even stronger when the aspect ratio is $\alpha = 5$. Another important observation is that for both aspect ratios, the apparent yield point is increased compared to the input value when taper is involved (the stress is calculated by using the area of the post top section; using an average area will result in early apparent yielding, and the post top area is easiest to measure experimentally). The simulations show that a propagation of the plastically deforming zone down the post axis is the cause of the spurious strain hardening and increased yielding point. In summary, the effects of taper are substantial and deleterious, and increase with post aspect ratio. Taper should therefore be avoided by careful manipulation of the micro-post fabrication process.

It is also found that for these prismatic posts with aspect ratio $\alpha = 5$ and no taper, buckling occurs even with friction considered. Higher-mode buckling is observed in this case, which is different from that when no friction is considered (the first-mode buckling). The observation of buckling in this case, unlike Fig. 4, is probably a result of the low strain hardening that has been assumed in Fig. 5. Thus large aspect ratio posts should also be avoided due to the possible occurrence of plastic buckling when one tests low strain hardening materials. We recommend post aspect ratios of 2–3 considering both the 2D and 3D simulation results from this study.

Finally we consider the effect of alignment of the system on the accuracy of μ-compression experiments. In this paper, we use the angle between the end-surface normal of the flat-end nano-indenter tip and the post axis to represent the misalignment. When this angle, θ, is 0, the system is perfectly aligned. We then examine the effect of various values of θ on the stress–strain outputs. Again we use the high-strength nano-crystalline nickel for input. The misalignment effect is manifested primarily in the deviation of the elastic part of the stress–strain curve, giving rise to an underestimate of the elastic modulus of the material. The effect of misalignment on measured elastic modulus is shown in Fig. 5(b). A decrease of the measured elastic modulus is observed with increase of misalignment (note that the lower elastic modulus even for perfect alignment ($\theta = 0°$) is due to the compliance of the post base, consistent with our 2D axisymmetric results presented in the previous section). In addition, excessive misalignment will result in buckling of the post. Therefore, care must be exercised to reduce or even eliminate misalignment in the system. In practice, FIB machining should allow one to control the end-surface of the flat-end indenter tip within $0.5°$. The uprightness of the posts should also be kept in mind in μ-compression sample preparation. Careful cleaning of the post-top is necessary to ensure the collinearity between the post and the end-surface normal of the indenter tip.

We note that the current micro-compression literature focuses primarily on specimens in which the anisotropy due to crystal plasticity is a dominant effect, and we have not considered this anisotropy. A subsequent paper presents results on effectively isotropic nano-crystalline materials obtained using this technique. We have also made no attempt in this paper to investigate size effects, whether arising from strain gradients or otherwise.

3. Conclusions

We have found that micro-compression tests can be used to faithfully measure the mechanical properties of certain materials. Our parametric study shows that:

1. Fillet radius/post radius ratios of 0.2–0.5 are recommended to provide sufficient test accuracy.
2. Strain hardening of the material significantly affects the μ-compression test accuracy, particularly when the fillet radius is large (close to the post radius).
3. From our 3D μ-compression simulations, for aspect ratios $\leqslant 5$, first-mode plastic buckling is suppressed by the friction between the indenter tip and the post top. We recommend post aspect ratios of 2–3.
4. Taper of the post results in overestimated elastic modulus, spurious strain hardening and increased apparent yield and thus should be minimized during micro-post fabrication.
5. Misalignment of the μ-compression system significantly affects the test accuracy by underestimating the elastic modulus, and may result in buckling of the post.

Acknowledgements

References

[1] Uchic MD, Dimiduk DM, Florando JN, Nix WD. Science 2004;305:986.
[2] Ma Q, Clarke DR. J Mater Res 1995;10:853.
[3] Uchic MD, Dimiduk DM, Florando JN, Nix WD. Mater Res Soc Symp Proc 2003;753:BB1.4.
[4] Greer JR, Oliver WC, Nix WD. Acta Mater 2005;53:1821.
[5] Gleiter H. Acta Mater 2000;48:1.
[6] Suryanarayana C. Int Mater Rev 1995;40:41.
[7] Kear BH, Colaizzi J, Mayo WE, Liao SC. Scripta Mater 2001;44:2065.
[8] Sharpe WN, Yuan B, Edwards RL. J Microelectromech S 1997;6:193.
[9] Ramberg W, Osgood WR. Technical Note 902. NACA, 1943.
[10] Chau KT. J Eng Mech 1997;123:1.
[11] Sneddon IN. Int J Eng Sci 1965;3:47.
[12] Wei Q, Ramesh KT, Ma E, Kesckes LJ, Dowding RJ, Kazykhanov VU, et al. Appl Phys Lett 2005;86:101907.
[13] Spear KE. J Am Ceram Soc 1989;72:171.
[14] Schuster BE, Ramesh KT, submitted for publication.

NO. OF
COPIES   ORGANIZATION

   1   DEFENSE TECHNICAL
 (PDF   INFORMATION CTR
 ONLY)   DTIC OCA
          8725 JOHN J KINGMAN RD
          STE 0944
          FORT BELVOIR VA 22060-6218

   1   US ARMY RSRCH DEV &
          ENGRG CMD
          SYSTEMS OF SYSTEMS
          INTEGRATION
          AMSRD SS T
          6000 6TH ST STE 100
          FORT BELVOIR VA 22060-5608

   1   INST FOR ADVNCD TCHNLGY
          THE UNIV OF TEXAS
          AT AUSTIN
          3925 W BRAKER LN
          AUSTIN TX 78759-5316

   1   DIRECTOR
          US ARMY RESEARCH LAB
          IMNE ALC IMS
          2800 POWDER MILL RD
          ADELPHI MD 20783-1197

   3   DIRECTOR
          US ARMY RESEARCH LAB
          AMSRD ARL CI OK TL
          2800 POWDER MILL RD
          ADELPHI MD 20783-1197

   3   DIRECTOR
          US ARMY RESEARCH LAB
          AMSRD ARL CS IS T
          2800 POWDER MILL RD
          ADELPHI MD 20783-1197

          ABERDEEN PROVING GROUND

   1   DIR USARL
          AMSRD ARL CI OK TP (BLDG 4600)

INTENTIONALLY LEFT BLANK.